The Sun and Heliosphere at Solar Maximum

E. J. Smith,[1] R. G. Marsden,[2] A. Balogh,[3] G. Gloeckler,[4] J. Geiss,[5] D. J. McComas,[6] R. B. McKibben,[7] R. J. MacDowall,[8] L. J. Lanzerotti,[9,10] N. Krupp,[11] H. Krueger,[12] M. Landgraf[2]*

Recent Ulysses observations from the Sun's equator to the poles reveal fundamental properties of the three-dimensional heliosphere at the maximum in solar activity. The heliospheric magnetic field originates from a magnetic dipole oriented nearly perpendicular to, instead of nearly parallel to, the Sun's rotation axis. Magnetic fields, solar wind, and energetic charged particles from low-latitude sources reach all latitudes, including the polar caps. The very fast high-latitude wind and polar coronal holes disappear and reappear together. Solar wind speed continues to be inversely correlated with coronal temperature. The cosmic ray flux is reduced symmetrically at all latitudes.

The space between the Sun and nearby stars is filled with ionized and neutral gas, dust, magnetic fields, and charged particles. The Sun excludes this pristine interstellar medium from a large volume called the heliosphere that completely encloses the planetary system. The Sun's influence extends to such great distances because the solar wind fills the heliosphere and exerts an outward pressure on the interstellar medium. The solar wind magnetic field keeps the low-energy interstellar plasma and magnetic field from penetrating into the heliosphere. However, interstellar neutrals, dust, and high-energy cosmic rays enter the heliosphere and their properties are altered by the solar wind, solar gravity, solar radiation, and charge exchange. The interaction between the Sun and the interstellar medium takes place not only at the outer boundary, but throughout the heliosphere.

Many space missions have explored the heliosphere near the solar equator, but only the Ulysses spacecraft has traveled from the equator to above the Sun's polar caps and extended our knowledge to a full three dimensions. The Ulysses orbit is inclined 80.2° to the solar equator, with a minimum solar distance (perihelion) beyond the orbit of Earth at 1.3 AU, a maximum distance (aphelion) of 5.3 AU, and a period of 6.3 years. The spacecraft, experiments, and observational results over the first complete orbit during 1992–1998 at sunspot minimum are described in (*1–4*). The second orbit, completed during the recent maximum in solar activity, produced the results reviewed below.

Magnetic Field

The solar/sunspot cycle is driven by changes in the Sun's magnetic field (*5*). At solar minimum, two opposing magnetic poles occupy the north and south polar caps. As solar maximum approaches, the poles decrease in strength and eventually vanish while very strong magnetic fields develop in sunspots and active regions. The polar cap fields reappear after many months but with their signs reversed; the field that was outward is now inward, and vice versa. The magnetic fields in the solar wind originate at the solar surface and must respond to the changing solar field.

At solar minimum, polar cap fields are a major source of the heliospheric magnetic field (HMF), dividing the heliosphere into two hemispheres in which the field has the same signs as the magnetic poles. The field remains in each hemisphere and does not cross into the other hemisphere or return to the Sun. Such fields with one end on the Sun and the other end extending out into the

[1]Jet Propulsion Laboratory, California Institute of Technology, Pasadena, CA 91109, USA. [2]Space Science Department of European Space Agency, European Space Technology Center, Postbus 299, 2200 AG Noordwijk, Netherlands. [3]Blackett Laboratory, Imperial College, London SW7 2BZ, UK. [4]Department of Physics, University of Maryland, College Park, MD 20742, USA. [5]International Space Science Institute, CH-3012 Bern, Switzerland. [6]Southwest Research Institute, San Antonio, TX 78238, USA. [7]Institute for the Study of Earth, Oceans and Space, University of New Hampshire, Durham, NH 03824, USA. [8]NASA Goddard Space Flight Center, Greenbelt, MD 20771, USA. [9]Bell Laboratories, Lucent Technologies, Murray Hill, NJ 07974, USA. [10]Center for Solar Terrestrial Research, New Jersey Institute of Technology, Newark, NJ 07021, USA. [11]Max Planck Institute for Aeronomy, D 37191 Katlenburg-Lindau, Germany. [12]Max Planck Institute for Kernphysik, 69029 Heidelberg, Germany.

*Present address: European Space Operations Center, 64293 Darmstadt, Germany.

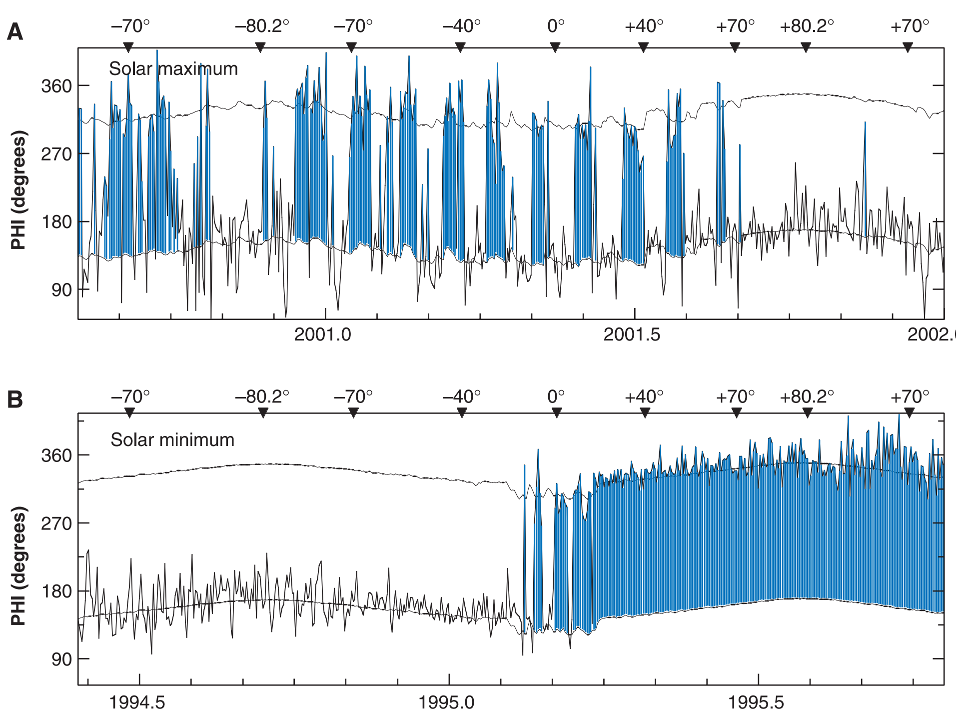

Fig. 1. Magnetic field spiral angle at minimum and maximum. The observed angle is plotted versus time, with heliographic latitude along the upper scale. (**A**) Observations during sunspot maximum; (**B**) observations during sunspot minimum. The observed angle agrees closely with predicted spiral angles (solid curves). At low latitudes, the angle switches rapidly between inward (white) and outward (blue) polarities. At high latitudes above the current sheet, only a single polarity is observed.

heliosphere are said to be "open." The heliospheric current sheet (HCS), which serves as the magnetic equator, separates the fields in the two hemispheres (*6*). The Sun's magnetic poles are generally not aligned with the rotation axis; as the Sun rotates, the HCS wobbles up and down, allowing fields above and below it to be observed, and the HMF appears to be divided into two "magnetic sectors." Because one end of the field rotates with the Sun while the other end is carried off by the solar wind, the field lines are not radial but form spirals.

The measured spiral angle φ_B (Fig. 1) is equal to Atan (B_ϕ/B_r), where the longitudinal and radial components of the magnetic field B_ϕ and B_r are in spherical polar coordinates. The figure also contains two theoretical curves based on the Parker model (*7*). For outward-directed fields, the Parker spiral is $\phi_P = -\Omega\ r \sin\theta/V$, where Ω is the angular rotation rate of the Sun, r is radial distance, θ is colatitude, and V is measured solar wind velocity. Inward fields lie along $\phi_P + \pi$. Variations in r, θ, and V cause ϕ_P to vary by ~20° with a minimum at the equator and a maximum at 80° latitude.

At solar minimum (Fig. 1B), the observed and model angles essentially agree at all latitudes. At latitudes above 40°, the field polarities have the same sign as in the polar caps. At lower latitudes, the HMF points outward for part of a solar rotation of ~25 days (the positive sector) and inward for the other part of the rotation (the negative sector). The HCS is located between the magnetic sectors at the changes in polarity and is also restricted to low latitudes.

At solar maximum (Fig. 1A), the observed and Parker angles again agree very closely. The two magnetic sectors extend to higher latitudes and single polarities only appear above ~70° latitude. The polarity in the south polar cap is inward, as at solar minimum, so the field has not yet reversed (*8*). In the north polar cap, the polarity is also inward; hence, the reversal has already occurred (*9*). Earth-based observations of the Sun indicate that the field in the south polar cap did not reverse until 2002.4, whereas the north polar cap reversed first in early 2001 (*10*). Thus, the Ulysses and solar observations are consistent, although their timing was not optimum. The reversal in the north polar cap occurred while Ulysses was in the southern hemisphere, and the reversal of the south pole took place while Ulysses was in the northern hemisphere.

The amount of open magnetic flux is measured by $B_r r^2$, the radial field component multiplied by the square of the radial distance. Ulysses has found that the open flux is independent of latitude at both minimum and maximum, with average values of $B_r r^2$ that are approximately the same in both phases (*9, 11, 12*) (fig. S1). Why the open flux varies so little with the solar cycle is puzzling. A recent theory suggests that the open flux may be invariant (*12, 13*).

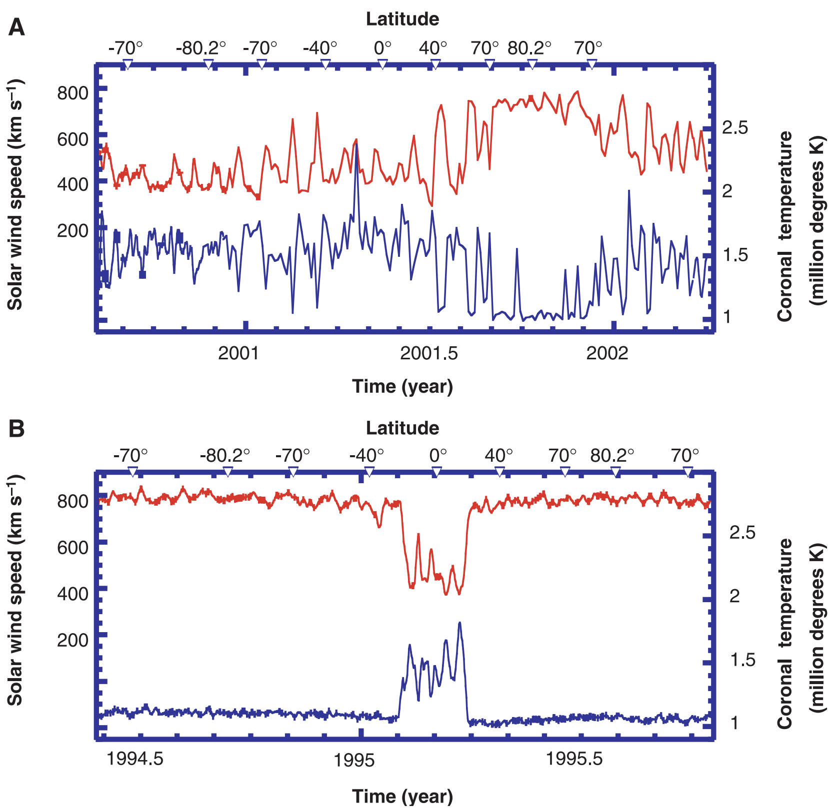

Fig. 2. Solar wind speed at minimum and maximum. The format and time intervals are the same as Fig. 1 with heliographic latitude along the upper scale. (**A**) Observations during sunspot maximum; (**B**) observations during sunspot minimum. Solar wind speed, V, is shown in red. Coronal temperature at the solar wind source, T_O (shown in blue), is anticorrelated with wind speed.

The absence of a dependence on latitude implies that the strong magnetic fields near the Sun force the solar wind to depart from strictly radial flow and cause the magnetic flux to become uniformly distributed. Once equilibrium is established at about 5 solar radii, the solar wind flow becomes radial (*11, 14*). Nonradial flow has important consequences for the solar wind and solar energetic particles, as discussed below.

The sector structure and the latitude independence of the open flux are properties that would be expected from two magnetic poles (i.e., a magnetic dipole), as modified by the solar wind. Presumably, the poles are located on a spherical "source" surface, enclosing the Sun, on which the field is radial, has a constant magnitude, and is inward above and outward below the HCS. The strength and the heliographic latitude and longitude of the poles can be inferred from HMF measurements (*12*).

Surprisingly, this simple source description is equally valid during both phases of the solar cycle. However, the magnetic poles are located in the polar caps at minimum and at low latitudes at maximum. (Alternatively, the inclination of the HCS is low at minimum and high at maximum.) A simplistic view is that the source dipole gradually rotates from an axial to an equatorial orientation, continuing toward the opposite heliographic pole to cause the change in the polarities of the polar caps. Of course, the changes in the solar magnetic field are actually much more complicated and are inconsistent with a simple rotating dipole (*12*). However, the open HMF does exhibit a structure and behavior that is very different and much less complicated than the "closed" fields (that begin and end on the Sun) that dominate the surface at solar maximum.

The major changes in the magnetic field affect all the heliospheric constituents including solar energetic particles and galactic cosmic rays, as discussed below. The distribution of low-mass interstellar dust also undergoes a solar cycle variation directly related to the changes in the HMF (*12, 15*) (fig. S2).

Solar Wind

The solar wind originates in discrete regions of the corona identified as coronal "holes," density depletions caused by the outflow (*16*). Throughout most of the solar cycle, two large coronal holes cover the polar caps while a few coronal holes occur at low and midlatitudes. Solar wind also originates near coronal "streamers," high-density structures pointing away from the Sun at high altitudes (*5*).

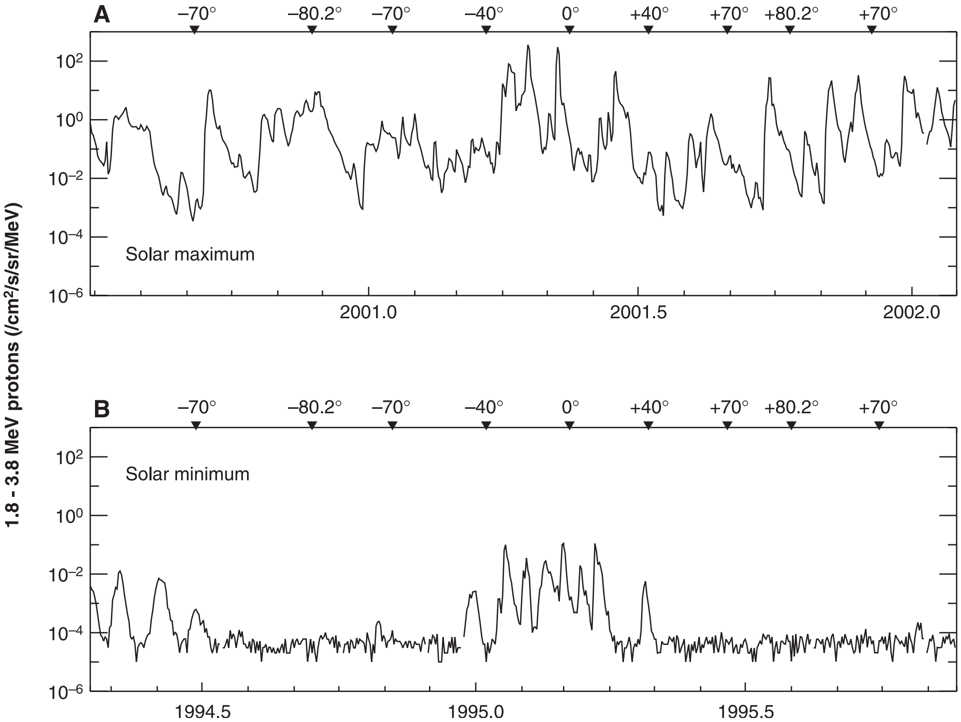

Fig. 3. Energetic particle flux at minimum and maximum. (**A**) Observations during sunspot maximum; (**B**) observations during sunspot minimum. The differential flux of protons with energies between 1.8 and 3.8 MeV is shown per unit solid angle (steradian) and unit energy interval (MeV). In (B), energetic particles are generally absent above ±40°. (The relatively constant values less than 10^{-4} of these units are noise.) In (A), elevated fluxes are present at all latitudes.

The two kinds of solar wind are evident in Fig. 2. At solar minimum (Fig. 2B), fast wind is continuously present at high latitudes (*19*). The variable slow wind is restricted to latitudes below ~20°. Solar wind structure is very different at maximum (Fig. 2A) (*20*). In the southern hemisphere, fast wind is absent and variable slow wind extends to all latitudes. In the northern hemisphere, several months later, fast wind is again observed above ~70° latitude (*21*). This south-north asymmetry is a solar cycle variation occurring while the spacecraft traveled between polar caps.

The disappearance and reappearance of fast wind is correlated with polar coronal holes (*10*). The south polar coronal hole disappeared by 2000.5, before Ulysses reached the south polar cap and found the absence of fast wind. The north polar coronal hole reappeared by 2001.4, before the spacecraft reached the north polar cap where it was immersed in fast high-latitude wind. In the southern hemisphere, the slow wind extended to the pole, although the sources were at lower latitudes (coronal holes and active regions). The nonradial expansion of the magnetic field explains how slow wind reached the polar cap.

Figure 2 also shows that V is inversely correlated with T_O throughout the solar cycle, including large variations in both parameters. T_O is proportional to $1/V^2$; when T_O decreases, V increases (*22*). In slow wind, $T_O \approx 1.5$ MK; in fast wind, $T_O \approx 1.0$ MK. Interestingly, this correlation does not hold for CMEs and provides another criterion, in addition to those already in use, to identify them.

The correlation relates a basic property of the corona to the solar wind speed. The inverse correlation was unexpected because it is contrary to models that depend on a pres-

Superposed on the background wind are episodic "coronal mass ejections" (CMEs) emitted by the Sun that pass through the heliosphere as self-contained volumes of plasma (*17*). CMEs originate in regions of closed magnetic fields including active regions, coronal streamers, and solar filaments (dark, ribbon-like structures) (*5*). Closed fields are often unstable and reconnect, releasing magnetized plasma to form a CME. As the CME accelerates to high speeds, a shock wave often forms and precedes it in the solar wind. A good example is a large CME observed in May 2001 while Ulysses was above the solar limb (*12*) (fig. S3).

The solar wind speed at Ulysses is shown in Fig. 2 (red curve) as a function of time and latitude. The figure also contains the electron temperature in the corona at the solar wind source (blue curve). Solar wind elements heavier than the dominant hydrogen and helium have different degrees of ionization depending on the number of electrons removed by collisions with hot coronal electrons. After the ions leave the corona, further ionization is negligible and observed "charge states" can be converted into the coronal electron temperature with the use of models (*18*). The temperature shown, T_O, is derived from oxygen ions.

Two kinds of solar wind are customarily distinguished on the basis of speed: relatively steady "fast wind" with speeds between ~600 and 800 km/s, and variable "slow wind" with speeds from 300 to 600 km/s. The distinction is useful because solar wind density and temperature are closely correlated with speed and because of interactions between fast and slow wind. When fast wind overtakes slow wind, a compression or interaction region (IAR) forms in which density, field strength, and pressure increase markedly. This high-pressure region expands, and eventually shock waves develop at the leading and trailing edges.

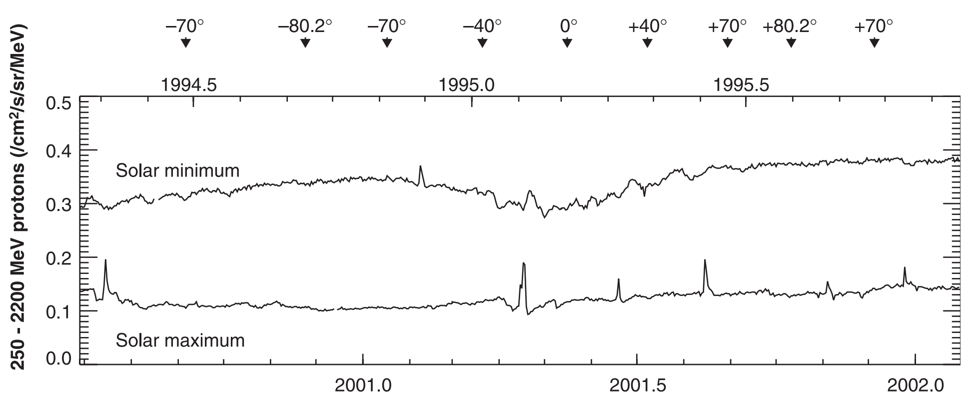

Fig. 4. Galactic cosmic rays at minimum and maximum. The flux of cosmic ray protons with energies between 250 and 2200 MeV is normalized to unit solid angle (steradian) and energy interval (MeV). In the upper curve (minimum), the decrease in flux between high and low latitudes is evidence of a dependence on latitude, with higher fluxes over the poles. At maximum, the average flux is reduced (a characteristic feature of the solar cycle), but no latitude gradient is evident. The "spikes" are the very energetic particles accelerated at the Sun in solar flares.

sure gradient in the corona to accelerate the solar wind such that higher temperatures should lead to faster, not slower, wind. The inverse relation is a new and powerful constraint to be met by all solar wind models. It has already led to a different type of model that emphasizes the role of the solar magnetic field (*23*).

Solar Energetic Particles

The heliosphere contains a distinct population of charged particles more energetic than the solar wind and less energetic than cosmic rays (*24*). They are solar particles accelerated near the Sun or out in the heliosphere. Particle acceleration in collisionless plasmas such as the solar wind occurs throughout the universe, and the study of solar energetic particles (SEPs) contributes to a general understanding of acceleration processes. SEPs are closely related to solar flares, CMEs, and solar wind IARs; all four vary with the solar cycle.

The SEPs in Fig. 3 are protons in the energy range 1.8 to 3.8 MeV (speeds from 6 to 9% of the speed of light). Their behavior is typical of particles at lower and higher energies present in these and other events. SEP events have a characteristic shape: an abrupt rise in intensity followed by a gradual decay. Near solar minimum (Fig. 3B), the particles are generally absent between 40° and 80° latitude. The quasi-periodic events below 40° are typical corotating interaction region (CIR) shock-related events. (The periodic increases in the south before 1994.5 are also associated with CIRs and are part of a long sequence that extends from the solar equator to high latitudes. No such events appear in the north polar cap, presumably because of decreasing solar activity.)

Major differences are evident at solar maximum (Fig. 3A). Energetic particles are continuously present at all latitudes, and their fluxes are orders of magnitude larger than at solar minimum (*25*). Large isolated events occur that do not repeat during the next solar rotation.

Events in Fig. 3 are similar to SEPs observed simultaneously in the ecliptic. However, the correlation at these low energies tends to be poor, with many more events being seen in the ecliptic than at Ulysses. However, higher energy SEPs (e.g., electrons with energies up to 1 MeV and protons up to 100 MeV) are more closely correlated with in-ecliptic events. The correlation is particularly striking during the decay phase, when the particle intensities are nearly the same despite large separations in latitude, longitude, and distance (*12*) (fig. S4). The particles evidently form a large "reservoir" in the inner heliosphere from which they slowly leak out (*26, 27*).

Many SEPs observed by Ulysses at high latitudes are associated with CMEs and IARs. The magnetic field and solar wind measurements show that they and their accompanying shocks are frequently present. Particle composition measurements confirm that they are the cause of some high-latitude SEPs (*28*). However, a different explanation is required for the presence of flare-associated SEPs at high latitudes and the formation of energetic particle reservoirs. The source of these particles is typically a specific active region at low latitudes. How are the particles able to reach high latitudes? How are they able to access all longitudes and fill the inner heliosphere?

The configuration of the HMF at solar maximum provides a possible explanation. As described above, the fields spread out to form a shell of constant magnetic flux near the Sun. Fields from low latitudes are diverted to high latitudes, and some reach the polar caps. Therefore, energetic particles produced at low latitudes can follow field lines to high latitudes.

Another possibility involves the effect on the energetic particles of fluctuations in the magnetic field. The magnetic field is turbulent, with persistent irregular variations in field direction superposed on the larger scale field. To SEPs traveling along the field, changes in direction are "scattering centers" that simultaneously retard particle motion along the field and cause them to move across field lines, a process similar to diffusion. The characteristic shape of SEP events is attributable to impulsive injection (the rapid rise) followed by diffusive propagation (the slow decay). Diffusion can explain how SEPs spread to all latitudes and longitudes to form the particle reservoirs. Cross-field diffusion appears to be more effective in the SEP events than had previously been anticipated, and a revised estimate of the diffusion coefficients may be needed to explain the Ulysses results.

Galactic Cosmic Rays

Cosmic rays are fully ionized atoms and electrons energized in distant parts of the galaxy and traveling at nearly the speed of light. Only some cosmic rays enter the heliosphere, where they interact with the HMF (*29, 30*). They encounter an outward-moving magnetic field, ever-present irregularities in the field direction, and varying curvature and magnitude of the HMF, and they lose energy as they struggle inward. As a result, the cosmic ray intensity decreases from the outer to the inner heliosphere. At sunspot maximum, fewer cosmic rays enter the heliosphere, a solar cycle variation referred to as "solar modulation." Understanding solar modulation is a major research goal and an essential step in relating cosmic rays inside and outside the heliosphere.

A basic issue for Ulysses was whether solar modulation is spherically symmetric or varies with latitude. Theorists predicted that, at minimum, cosmic rays would have easier access to the polar caps because the magnetic field is less spiraled and the paths taken by the cosmic rays are shorter. Furthermore, cosmic rays encountering the HCS drift outward and escape. Therefore, a large-scale circulation of the cosmic rays was expected that was inward at high latitudes and outward at low latitudes, with higher particle flux at high latitudes.

At minimum (Fig. 4), the flux at high energies (e.g., 250- to 2000-MeV protons) is indeed ~30% greater in the polar caps than near the equator (*31, 32*). Theoretical models successfully related this gradient to drifts, but high-latitude access was limited by large-amplitude magnetic fluctuations whose presence was confirmed by Ulysses (*33, 34*).

Theorists had difficulty predicting what Ulysses would find at solar maximum without knowing the properties of the magnetic field at high latitudes. As expected (Fig. 4), the flux of cosmic rays was reduced by a factor of ~3 as a result of solar modulation. However, the difference between the equator and the poles was essentially nonexistent (*35, 36*). The cosmic rays showed little if any effect of drifts, and the modulation was spherically symmetric.

References and Notes

1. E. J. Smith, R. G. Marsden, D. E. Page, *Science* **268**, 1005 (1995).
2. E. J. Smith, R. G. Marsden, *Geophys. Res. Lett.* **22**, 3297 (1995).
3. R. G. Marsden, E. J. Smith, J. F. Cooper, C. Tranquille, *Astron. Astrophys.* **316**, 279 (1996).
4. A. Balogh, R. G. Marsden, E. J. Smith, Eds., *The Heliosphere Near Solar Minimum: The Ulysses Perspective* (Springer-Praxis, London, 2001).
5. P. V. Foukal, *Solar Astrophysics* (Wiley, New York, 1990).
6. E. J. Smith, *J. Geophys. Res.* **106**, 15819 (2001).
7. E. N. Parker, *Interplanetary Dynamical Processes* (Interscience, New York, 1963).
8. E. J. Smith, A. Balogh, R. J. Forsyth, D. J. McComas, *Geophys. Res. Lett.* **28**, 4159 (2001).
9. E. J. Smith, A. Balogh, in *Solar Wind Ten*, M. Velli, R. Bruno, F. Malara, Eds. (American Institute of Physics, Melville, NY, 2003), p. 67.
10. K. L. Harvey, F. Receley, *Solar Phys.* **211**, 31 (2002).
11. E. J. Smith, A. Balogh, *Geophys. Res. Lett.* **22**, 3317 (1995).
12. See supporting text on *Science* Online.
13. L. A. Fisk, N. A. Schwadron, *Space Sci. Rev.* **97**, 21 (2001).
14. S. T. Suess, E. J. Smith, *Geophys. Res. Lett.* **23**, 3267 (1996).
15. M. Landgraf, *J. Geophys. Res.* **105**, 10303 (2000).
16. J. B. Zirker, *Coronal Holes and High Speed Streams* (Colorado Assoc. Univ. Press, Boulder, CO, 1977).
17. N. Crooker, J. A. Joselyn, J. Feynman, Eds., *Coronal Mass Ejections,* Geophysical Monongraph 99 (American Geophysical Union, Washington, DC, 1997).
18. Y.-K. Ko, L. A. Fisk, J. Geiss, G. Gloeckler, M. Guhathakurta, *Solar Phys.* **171**, 345 (1997).
19. M. Neugebauer, in *The Heliosphere Near Solar Minimum: The Ulysses Perspective,* A. Balogh, R. G. Mars-

den, E. J. Smith, Eds. (Springer-Praxis, London, 2001), pp. 43–106.
20. D. J. McComas *et al.*, *Geophys. Res. Lett.* **29** (9), 10.1029/2001GL013940 (2002).
21. D. J. McComas *et al.*, *Geophys. Res. Lett.* **30** (10), 10.1029/2003GL017136 (2003).
22. G. Gloeckler, T. H. Zurbuchen, J. Geiss, *J. Geophys. Res.* **108**, 10.1029/2002JA009286 (2003).
23. L. A. Fisk, *J. Geophys. Res.* **108**, 10.1029/2002JA009284 (2003).
24. L. J. Lanzerotti, T. R. Sanderson, in *The Heliosphere Near Solar Minimum: The Ulysses Perspective,* A. Balogh, R. G. Marsden, E. J. Smith, Eds. (Springer-Praxis, London, 2001), pp. 259–286.
25. G. M. Simnett, *Space Sci. Rev.* **97**, 231 (2001).
26. R. B. McKibben, C. Lopate, M. Zhang, *Space Sci. Rev.* **97**, 257 (2001).
27. E. C. Roelof *et al.*, *Geophys. Res. Lett.* **19**, 1243 (1992).
28. M. Y. Hofer *et al.*, *Geophys. Res. Lett.* **29** (16), 10.1029/2002GL014944 (2002).
29. R. B. McKibben, in *The Heliosphere Near Solar Minimum: The Ulysses Perspective,* A. Balogh, R. G. Marsden, E. J. Smith, Eds. (Springer-Praxis, London, 2001), pp. 327–371.
30. L. A. Fisk *et al.*, Eds., *Cosmic Rays in the Heliosphere* (Kluwer Academic, Dordrecht, Netherlands, 1998).
31. J. Simpson, M. Zhang, S. Bame, *Astrophys. J.* **465**, L69 (1996).
32. B. Heber *et al.*, *Astron. Astrophys.* **316**, 538 (1996).
33. J. R. Jokipii *et al.*, *Geophys. Res. Lett.* **22**, 3385 (1995).
34. M. S. Potgieter, *Space Sci. Rev.* **83**, 147 (1998).
35. R. B. McKibben, C. Lopate, M. Zhang, *Space Sci. Rev.* **97**, 367 (2001).
36. B. Heber, R. G. Marsden, *Space Sci. Rev.* **97**, 309 (2001).
37. Work presented here was performed by the Jet Propulsion Laboratory of the California Institute of Technology under a contract with NASA.

Supporting Online Material
www.sciencemag.org/cgi/content/full/302/5648/1165/DC1
SOM Text
Figs. S1 to S4